AIP Journal of Applied Physics

Temperature dependence of piezoelectric properties of high- T C Bi (Mg 1 / 2 Ti 1 / 2) O 3 – PbTiO 3

Jun Chen, Xiaoli Tan, Wook Jo, and Jürgen Rödel

Citation: Journal of Applied Physics **106**, 034109 (2009); doi: 10.1063/1.3191666

View online: http://dx.doi.org/10.1063/1.3191666

View Table of Contents: http://scitation.aip.org/content/aip/journal/jap/106/3?ver=pdfcov

Published by the AIP Publishing

Temperature dependence of piezoelectric properties of high-T_C $Bi(Mg_{1/2}Ti_{1/2})O_3-PbTiO_3$

Jun Chen,[1,a] Xiaoli Tan,[2] Wook Jo,[1] and Jürgen Rödel[1]
[1]*Institute of Materials Science, Technische Universität Darmstadt, Petersenstr. 23, 64287 Darmstadt, Germany*
[2]*Department of Materials Science and Engineering, Iowa State University, Ames, Iowa 50011, USA*

(Received 15 April 2009; accepted 4 July 2009; published online 10 August 2009)

The temperature dependence of both polarization and electric-field induced strain was investigated for $(1-x)Bi(Mg_{1/2}Ti_{1/2})O_3-xPbTiO_3$ ($x=0.36$, 0.37, and 0.38), with the morphotropic phase boundary located at $x=0.37$. Remanent polarization (P_r) and maximum polarization (P_{max}) of all compositions are enhanced with increasing temperature up to 175 °C, which is rationalized as improved domain switching due to reduced tetragonality (c/a). The hysteresis during unipolar electric cycling tends to decrease with increase in the fraction of tetragonal phase. Temperature dependent x-ray diffraction demonstrates that switched non-180° domains are stable against thermal depoling above 200 °C, which indicates that the currently investigated materials are suitable for high temperature applications. This promising high-T_C piezoelectric is further discussed with reference to oxygen octahedron of the tilted $R3c$ and untilted $R3m$ space groups and the tolerance factor (t). © *2009 American Institute of Physics*. [DOI: 10.1063/1.3191666]

I. INTRODUCTION

Over the past decade, a great demand has been raised for piezoelectric materials for usage at temperatures as high as possible, especially in the aerospace and automotive industries.[1–3] The operating temperature of piezoelectric ceramics is generally limited to one-half of the Curie point (T_C) due to loss of polarization, typically at temperatures lower than 200 °C [e.g., 150 °C for the conventional piezoelectric materials based on the $Pb(Zr_{1-x}Ti_x)O_3$ (PZT)] with a Curie temperature, $T_C=386$ °C.[4]

After excellent piezoelectric properties for $(1-x)BiScO_3-xPbTiO_3$ (BS-PT) near the morphotropic phase boundary (MPB) ($x=0.64$) were reported (piezoelectric coefficient, $d_{33}=460$ pC/N, planar coupling coefficient, $k_p=0.56$, and $T_C=450$ °C) recently,[5,6] the discovery of several promising high temperature piezoelectric materials with high performance followed in the general $BiMeO_3-PbTiO_3$ system,[5–24] where Me can be a single cation of valency +3 (e.g., Sc^{3+} and Fe^{3+}) or a mixture of cations with an average valence of +3 (e.g., $Mg_{1/2}Ti_{1/2}$ and $Ni_{2/3}Nb_{1/3}$). It has been proposed that the Bi substitution plays an unusual role of considerable enhancement of both Curie temperature (T_C) and tetragonality (c/a), which results from a strong coupling between Pb/Bi cations and *B*-site cations of strong ferroelectric activity, such as Ti, Zn, and Fe.[25]

Although BS-PT shows good piezoelectric properties even superior to the conventional PZT-based piezoceramics, its market application is highly restricted by the high price of Sc_2O_3. Hence, most recent studies have been focusing on nonscandium perovskites.[12–24] In fact, possible new compositions in $BiMeO_3-PbTiO_3$-based systems are plenty, because *B*-site Me of $BiMeO_3$ could be any combination, which gives an average valence of +3. According to the currently available literature, however, the design of $BiMeO_3-PbTiO_3$ piezoelectrics faces a significant challenge in that only few systems form a MPB with $PbTiO_3$. Most $BiMeO_3$ compounds show limited solubility in $PbTiO_3$ such that the MPB is rarely reached. This has been demonstrated in such systems as $Bi(Zn_{1/2}Ti_{1/2})O_3-PbTiO_3$ (BZT-PT) and $Bi(Zn_{2/3}Nb_{1/3})O_3-PbTiO_3$.[7,20–24] Table I lists the piezoelectric and related properties of $BiMeO_3-PbTiO_3$ piezoceramics available in literature. It should be noted that most $BiMeO_3-PbTiO_3$ compositions have a relatively high T_C. However, except BS-PT,[6] $Bi(Ni_{1/2}Ti_{1/2})O_3-PbTiO_3$ (Ref. 12) and $Bi(Mg_{1/2}Ti_{1/2})O_3-PbTiO_3$,[13] all known $BiMeO_3-PbTiO_3$-based systems have low or inferior piezoelectric properties at their MPB. As $Bi(Ni_{1/2}Ti_{1/2})O_3-PbTiO_3$ suffers from high conductivity and dielectric losses,[12] we chose $Bi(Mg_{1/2}Ti_{1/2})O_3-PbTiO_3$ for our current study.

For consideration as high-T_C piezoelectric, the temperature dependence of piezoelectric properties is most crucial for applications such as actuators and sensors. However, most studies so far have been related only to structure, ferroelectric, and piezoelectric properties at room temperature, with few exceptions.[14,26] In this study, therefore, ceramics of $(1-x)Bi(Mg_{1/2}Ti_{1/2})O_3-xPbTiO_3$ near the MPB ($x=0.36$, 0.37, and 0.38) were prepared by the conventional solid-state method to investigate the temperature dependence of polarization and strain of bipolar and unipolar electric loading. These are then correlated with the crystal structures as determined by high temperature x-ray diffraction (XRD).

II. EXPERIMENT

$(1-x)Bi(Mg_{1/2}Ti_{1/2})O_3-xPbTiO_3$ (abbreviated as BMT-PT100x) ceramics of three compositions ($x=0.36$, 0.37, and 0.38) were prepared by the conventional solid-state reaction method. $MgTiO_3$ was first synthesized as a precur-

[a]Author to whom correspondence should be addressed. Electronic mail: junchen@metall.ustb.edu.cn.

TABLE I. Piezoelectric and related properties of $(1-x)BiMeO_3-xPbTiO_3$ in the composition near the MPB. The ceramics are sorted by the value of d_{33} in descending order.

Compound	MPB (mol % PT)	T_C (°C)	d_{33} (pC/N)	k_p	tan δ	E_C (kV/mm)	c/a	Ref.
$0.36BiScO_3-0.64PbTiO_3$	64	450	460	0.56	0.027	2.0	1.023	5
$0.45Bi(Sc_{1/2}Fe_{1/2})O_3-0.55PbTiO_3$	55	440	298	0.49	0.033	2.2	1.021	9
$0.51Bi(Ni_{1/2}Ti_{1/2})O_3-0.49PbTiO_3$	49	400	260	⋯	⋯	3.8	1.018	12
$0.63Bi(Mg_{1/2}Ti_{1/2})O_3-0.37PbTiO_3$	37	478	225	⋯	0.063	5.0	1.034	13 and 15
$0.60(Bi_{0.9}La_{0.1})(Fe_{0.95}Ga_{0.05})O_3-0.40(Pb_{0.9}Ba_{0.1})TiO_3$	40	386	186	0.37	0.04	2.8	1.030	16
$0.38Bi(Mg_{3/4}W_{1/4})O_3-0.62PbTiO_3$	62	220	150	⋯	0.046	4.2	1.002	17 and 18
$0.35Bi(Ni_{2/3}Nb_{1/3})O_3-0.65PbTiO_3$	65	273	140	0.22	0.11	2.8		19
$0.4Bi(Sc_{3/4}Ga_{1/4})O_3-0.6PbTiO_3$	60	477	124	⋯	0.05	3.9	1.027	10
$0.33(Bi_{0.7}La_{0.3})(Zn_{0.15}Mg_{0.35}Ti_{0.5})O_3-0.67PbTiO_3$	⋯	300	94	⋯	⋯	4.7	1.030	20
$0.15BiInO_3-0.85PbTiO_3$(1.5 mol % Nb_2O_5)	⋯	542	60	0.11	0.014	12.5	1.067	21

sor at 1400 °C for 4 h using reagent graded oxide precursors[13,15] and then mixed with PbO (99.9%, Alfa Aesar), TiO_2 (99.9%, Alfa Aesar), and Bi_2O_3 (99.975%, Alfa Aesar) according to the stoichiometric formulas of each composition. These powder mixtures were ball milled in ethanol for 12 h. Calcination at 850 °C for 5 h was then followed by renewed ball milling for another 12 h. Calcined powders were uniaxially pressed into pellets with a diameter of 10 mm and thickness of ~1 mm, and then hydrostatically compacted at 200 MPa. The green compacts were embedded in the calcined powders of the same composition, and sintered in a covered crucible at 1100 °C for 2 h.

XRD (STOE STADI P) at room temperature was performed to reveal the crystal structures. The temperature dependence of the crystal structure of poled pellets of BMT-PT38 was further studied from room temperature to 325 °C (Bruker Siemens D8). The data were collected in 2θ angular range of 20°–60° using a step (0.02°) scanning mode with step duration of 5 s. The diffraction patterns were calculated with the software FULLPROF. For electrical measurements, sintered pellets were ground and polished to a thickness of ~0.5 mm. The polished samples were electroded with silver paste and then fired at 550 °C for 30 min. A triangular waveform at a frequency of 1 Hz was applied to monitor the temperature dependence of polarization (P) and field-induced longitudinal strain (S) curves in a silicone oil bath by using a Sawyer–Tower circuit equipped with a strain gauge. The measurement was performed from room temperature to 175 °C with an interval of 25 °C. Before collecting data for each temperature, the sample was held at each specified temperature for 30 min to minimize thermal fluctuation. For the temperature dependent XRD and the measurement of the small-signal piezoelectric coefficient d_{33}, samples were poled at 120 °C under an electric field of 5 kV/mm for a dwell time of 10 min, and cooled down to room temperature under the applied electric field. After 24 h aging of the poled sample, the d_{33} value was measured using a Berlincourt meter (YE 2730, Sinocera, Shanghai, China).

III. RESULTS AND DISCUSSION

$(1-x)Bi(Mg_{1/2}Ti_{1/2})O_3-xPbTiO_3$ forms a solid solution in a wide range of compositions, with $0.3 \le x \le 1.0$.[13] The solubility limit of BMT (70 mol %) is considerably higher than the other types of $(1-x)BiMeO_3-xPbTiO_3$, e.g., 40 mol % of BS for BSPT,[6] and 35 mol % of BZT for BZT-PT.[22] The room temperature XRD patterns of $(1-x)Bi(Mg_{1/2}Ti_{1/2})O_3-xPbTiO_3$ near the MPB (x=0.36, 0.37, and 0.38) are shown in Fig. 1(a). These are consistent with a perovskite structure for all three compositions without any trace of secondary phases. BMT-PT38 is indexed as tetragonal with the apparent splitting between (002) and (200) diffraction peaks, while BMT-PT36 is predominantly rhombohedral with a small amount of tetragonal phase. Both rhombohedral and tetragonal symmetries are present in BMT-PT37.[13] From a structural point of view, therefore, the MPB that consists of tetragonal (T, space group: $P4mm$) and rhombohedral (R, space group: $R3c$) phases is determined to

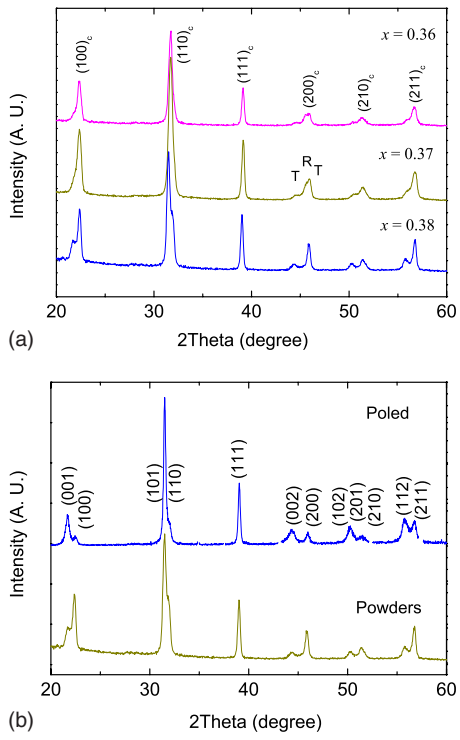

FIG. 1. (Color online) (a) XRD patterns of $(1-x)Bi(Mg_{1/2}Ti_{1/2})O_3-xPbTiO_3$ (x=0.36, 0.37, and 0.38) at room temperature. (b) XRD patterns of the powder and a poled ceramic pellet of $0.62Bi(Mg_{1/2}Ti_{1/2})O_3-0.38PbTiO_3$.

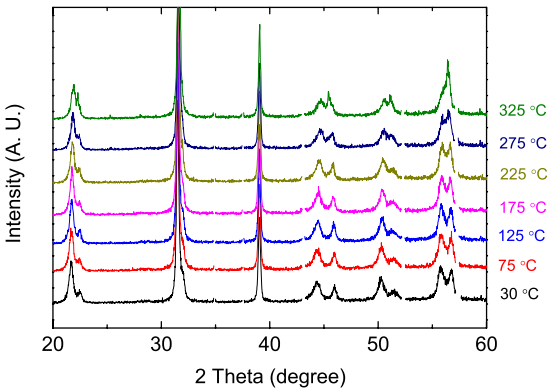

FIG. 2. (Color online) Temperature dependence of XRD patterns of a poled pellet of $0.62Bi(Mg_{1/2}Ti_{1/2})O_3-0.38PbTiO_3$.

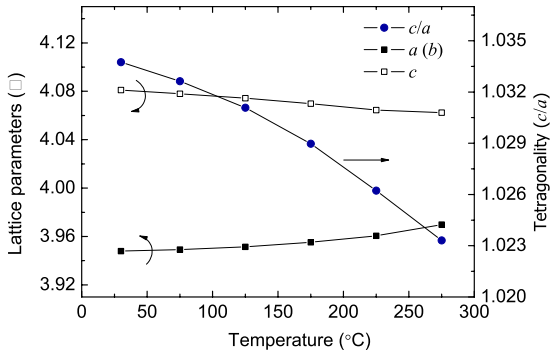

FIG. 3. (Color online) Lattice parameters (Å) and tetragonality (c/a) as functions of temperature for $0.62Bi(Mg_{1/2}Ti_{1/2})O_3-0.38PbTiO_3$.

be in the range of $x=0.36-0.37$. The lattice parameters of tetragonal BMT-PT38 were obtained as a $(b)=3.947(9)$ Å and $c=4.081(1)$ Å, yielding a tetragonality $(c/a=1.034)$ at the tetragonal side of the MPB, which is among the largest in $(1-x)BiMeO_3-xPbTiO_3$ materials (see Table I). Figure 1(b) depicts the room temperature XRD patterns of tetragonal BMT-PT38 recorded from powders and a poled pellet. A poling-induced texture can be clearly seen from the intensity change in (002) and (200) peaks at around $2\theta=45°$, corresponding to the spontaneous polarization directions of the tetragonal ferroelectric phase.

The temperature dependence of the crystal structure and the thermal stability of polarization were assessed by high temperature XRD on a poled pellet after removal of the silver electrodes. Figure 2 exemplarily shows high temperature XRD patterns from BMT-PT38 in the temperature range of RT to 325 °C with an interval of 50 °C. In the temperature range of RT to 275 °C, BMT-PT38 mainly preserves its tetragonal structure. It is interesting to note that there is no noticeable change in the ratio between the intensities of (002) and (200), which indicates that the switched domains have a good thermal stability in the investigated temperature range essential for a promising candidate for high temperature piezoelectric applications. However, when temperature was further increased to 325 °C, several new diffraction peaks that can be indexed as a pseudocubic phase appear, indicating that a phase transition takes place at around this temperature. An additional peak was also observed at 300–400 °C in the temperature dependence of dielectric constant measurement.[14] The nature of this phase transition at this temperature is not yet understood and subject to further investigations.

The lattice constants of the tetragonal phase are presented in Fig. 3. With increasing temperature, the a (b) axis increases while the c axis decreases, resulting in a reduced c/a. A reduced c/a ratio translates into a reduced internal stress level, which is expected to alleviate further domain switching.

The temperature dependence of $P(E)$ and $S(E)$ from room temperature to 175 °C for $(1-x)Bi(Mg_{1/2}Ti_{1/2})O_3-xPbTiO_3$ $(x=0.36, 0.37,$ and $0.38)$ is depicted in Figs. 4–6. The $P(E)$ and $S(E)$ curves of all three compositions display an archetypal shape for normal ferroelectrics such as PZT. The important ferroelectric properties at room temperature are close to those reported in literature[13] and are summarized in Table II. When compared with the other typical systems listed in Table I, E_C of BMT-PT is comparatively high, which could be attributed to its large tetragonality (c/a) and hence large internal stress level. This is consistent with a decrease in E_C as the amount of tetragonal phase is replaced by rhombohedral phase (see Table II). The lattice distortion of the tetragonal phase, given by $\delta t=(c/a-1)$ with 3.4% for BMT-PT38, is larger in this system than that of the rhombohedral phase, given by $\delta r=(9/8)(d_{111}/d_{-111}-1)$ with 0.45% for BMT-PT36.[27] The different behavior between δt and δr holds also true in other ferroelectric systems, representatively in PZT.[27]

As shown in Figs. 4–6, the coercive field (E_C) is decreased as the temperature increases, but P_{max} (polarization at maximum field) and P_r (remanent polarization) were observed to increase with temperature. Temperature dependent polarization and strain are similar between the three compositions. All are enhanced with temperature within the investigated temperature range. At 175 °C, polarization is slightly effected by an increased conductivity. Note that the influence of temperature on polarization is quite different to that of normal ferroelectric materials. Commonly, polarization values decrease continuously up to the Curie temperature (T_C).[28–30] This unusual behavior is rationalized by the fact that the poling field of 8 kV/mm does not suffice to fully pole BMT-PT near room temperature possibly due to severe domain wall locking from its high c/a ratio. The enhanced polarization values at increased temperature are thus ascribed to an increase in the amount of switchable non-180° domains, caused by a reduced E_C.

The increase in the total strain with temperature can be explained in a similar manner. For ferroelectric materials, the total strain is provided by a combination of intrinsic piezoelectric effect (lattice straining) and extrinsic piezoelectric effect (domain switching). The intrinsic piezoelectric effect is not expected to increase with decreasing c/a ratio stemming from the increase in temperature (Fig. 3). Hence, the enhancement of electric-field induced strain and polarization is attributed to enhanced domain switching. This is also evident from the changes in the negative strain, which is defined as the difference between the strain at zero electric field and the minimum strain during bipolar cycles.[29] Note that the

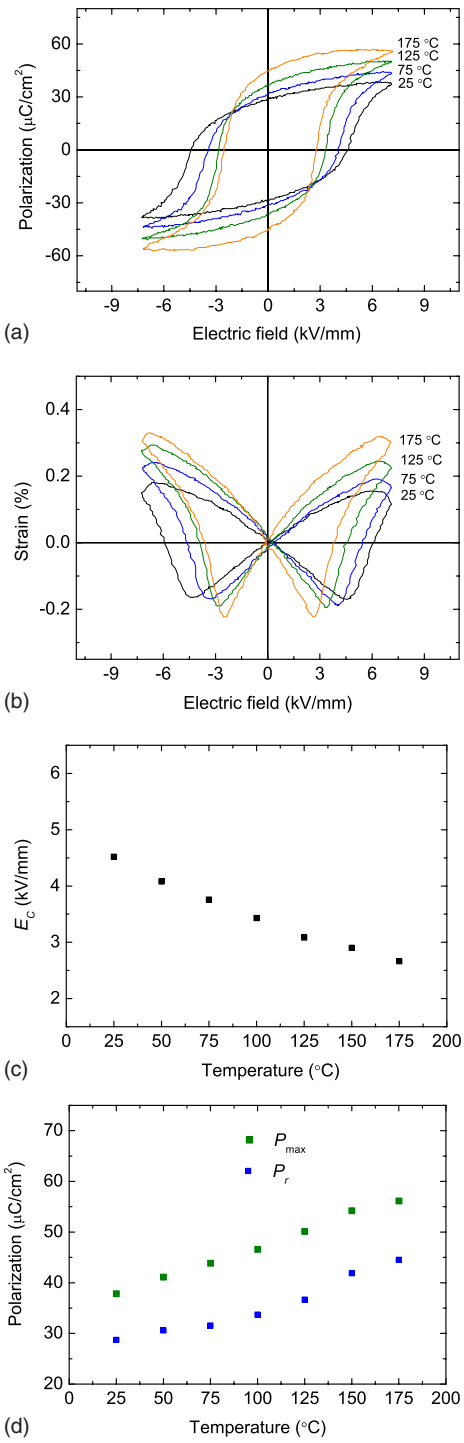

FIG. 4. (Color online) Temperature dependence of (a) $P(E)$ loops, (b) bipolar $S(E)$ curves, (c) E_C, and (d) polarization for $0.64Bi(Mg_{1/2}Ti_{1/2})O_3-0.36PbTiO_3$.

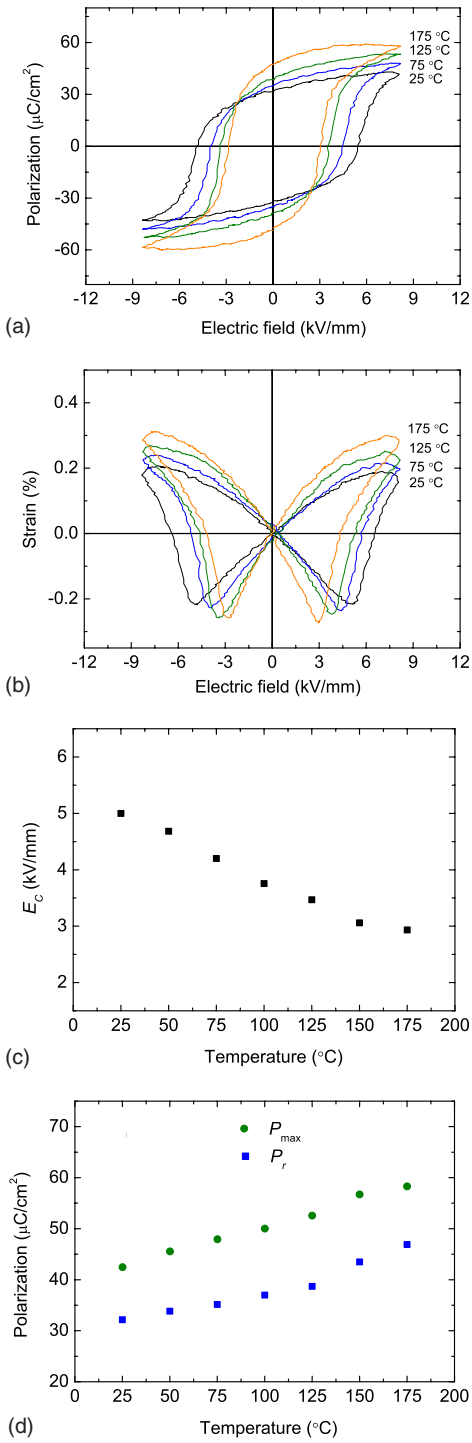

FIG. 5. (Color online) Temperature dependence of (a) $P(E)$ loops, (b) bipolar $S(E)$ curves, (c) E_C, and (d) polarization for $0.63Bi(Mg_{1/2}Ti_{1/2})O_3-0.37PbTiO_3$.

negative strain becomes even larger with a reduced c/a, and the strain minimum occurs at a lower electric field as the temperature increases. Note that in bulk PZT, both total strain and negative strain decrease with rising temperature, following the reduced lattice distortion.[31]

If application as an actuator for high temperature is contemplated for BMT-PT piezoceramics, then the electric-field induced unipolar strain is an essential parameter (Fig. 7). There is a clear distinction between the compositions containing dominantly rhombohedral and tetragonal crystal structures. The strain of BMT-PT38 increases almost in linear fashion, while the $S(E)$ unipolar curve of BMT-PT36 bends upward. Strain hysteresis can be quantified as a ratio of the difference between up-poling and down-poling strains at a half maximum electric field to the total strain at the maximum field.[32] At room temperature, for example, the hysteresis of BMT-PT36 (51%) at 7 kV/mm is almost two times larger than that of BMT-PT38 (24%). This supports the previous assumption that the high lattice distortion is responsible for the limited contribution from domain switching,

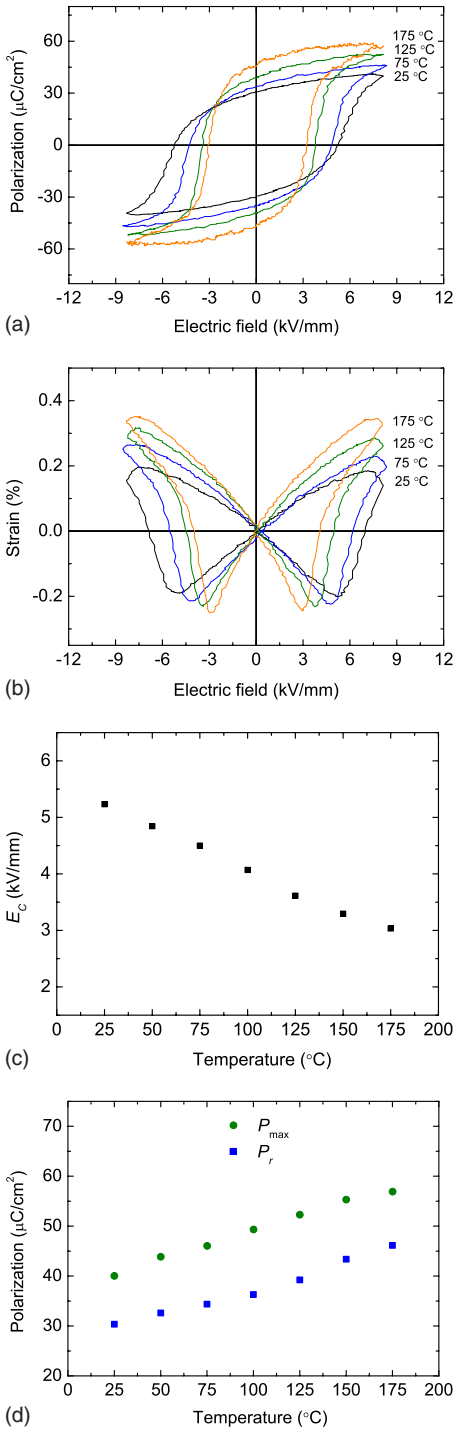

FIG. 6. (Color online) Temperature dependence of (a) $P(E)$ loops, (b) bipolar $S(E)$ curves, (c) E_C, and (d) polarization for $0.62Bi(Mg_{1/2}Ti_{1/2})O_3-0.38PbTiO_3$.

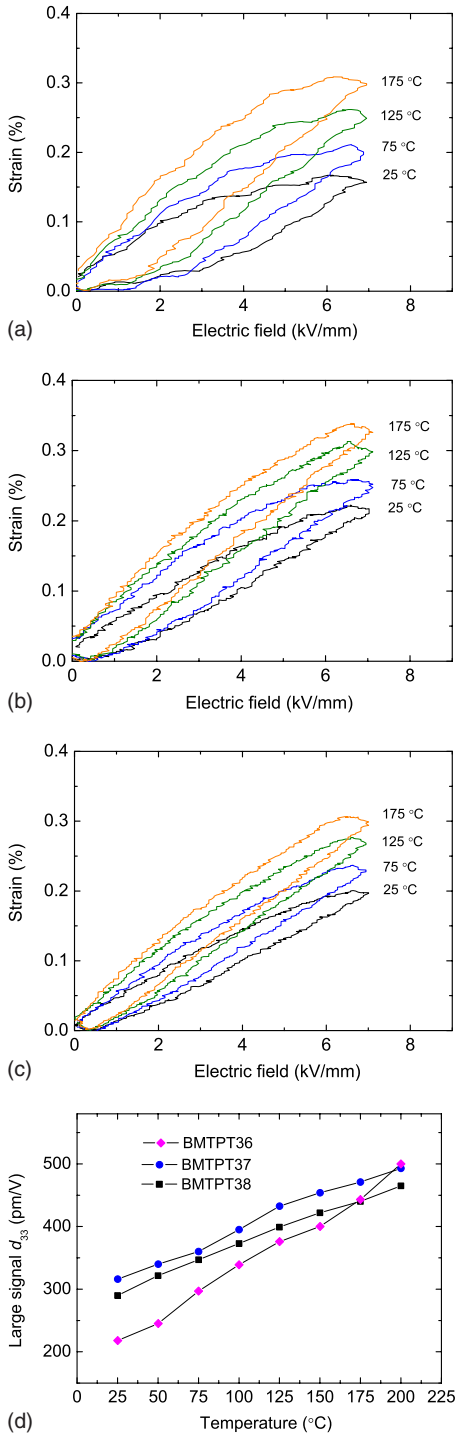

FIG. 7. (Color online) Temperature dependence of unipolar $S(E)$ curves of $(1-x)PbTiO_3-xBi(Mg_{1/2}Ti_{1/2})O_3$, (a) $x=0.36$, (b) $x=0.37$, (c) $x=0.38$, and (d) large signal d_{33}.

TABLE II. Room temperature ferroelectric properties of $(1-x)Bi(Mg_{1/2}Ti_{1/2})O_3-xPbTiO_3$ at 8 kV/mm.

Composition (x)	E_C (kV/mm)	P_{max} ($\mu C/cm^2$)	P_r ($\mu C/cm^2$)
$0.64Bi(Mg_{1/2}Ti_{1/2})O_3-0.36PbTiO_3$	4.7	44.1	33.2
$0.63Bi(Mg_{1/2}Ti_{1/2})O_3-0.37PbTiO_3$	5.0	42.5	32.4
$0.62Bi(Mg_{1/2}Ti_{1/2})O_3-0.38PbTiO_3$	5.3	39.7	30.2

since the lattice distortion is smaller in the rhombohedral phase in BMT-PT. A reduced lattice distortion then prompts increased levels of domain switching and increased hysteresis [Fig. 7(a)]. Figure 7(d) provides the large-signal d_{33} (S_{max}/E_{max}) as a figure of merit for actuator applications. S_{max}/E_{max} for all three compositions shows a linear increase with temperature.

Large and small signal d_{33} values at room temperature are presented in Fig. 8. The large signal d_{33} is about 20%–40% larger than the small signal one, which can be compared

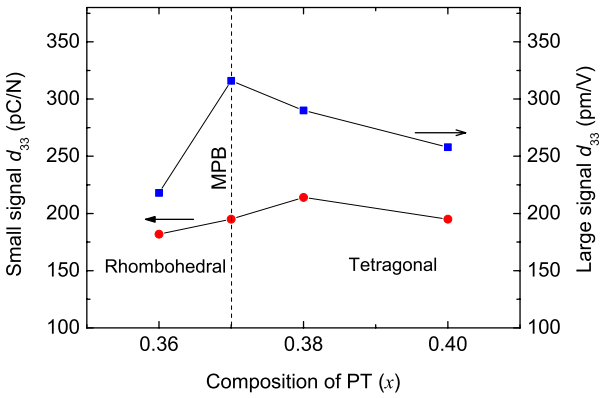

FIG. 8. (Color online) Piezoelectric coefficient d_{33} of $(1-x)$Bi$(Mg_{1/2}Ti_{1/2})O_3-xPbTiO_3$.

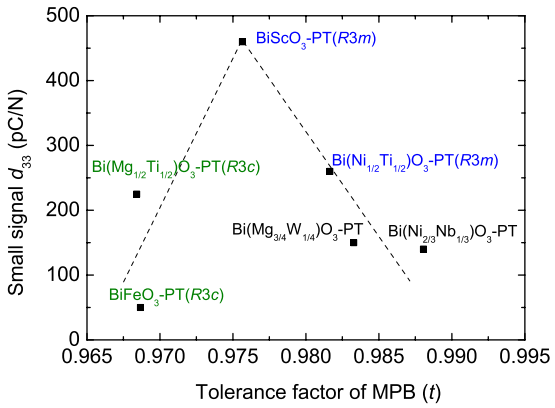

FIG. 9. (Color online) Small signal d_{33} value as a function of tolerance factor (t) at MPB in typical $BiMeO_3-PbTiO_3$ piezoelectric ceramics. The dashed lines are guide for the eyes and suggest a possible trend. The space group of the rhombohedral phase is not reported for $Bi(Mg_{3/4}W_{1/4})O_3-PbTiO_3$ and $Bi(Ni_{2/3}Nb_{1/3})O_3-PbTiO_3$.

to soft PZT, where this value is at about 50%.[32] The deviation is larger on the tetragonal side of the MPB than on the rhombohedral side, though the extrinsic contribution to the electric-field induced strain seems larger in the rhombohedral side as was discussed above (see Fig. 7). This suggests that non-180° domain switching in rhombohedral symmetry is less effective in enhancing the total strain level.

According to literature, the piezoelectric properties of BMT-PT depend strongly on processing route.[13–15] BMT-PT can be obtained with high d_{33} (225 pC/N) and large dielectric breakdown field using hot isostatic pressing.[13] Conventional processing leads to problems with respect to high conductivity[14,15] and low dielectric breakdown strength (5 kV/mm).[14] The piezoelectric coefficient (small signal d_{33} = 166 pC/N) is lower when using the one-step conventional process without employing $MgTiO_3$ as a precursor.[14] Note that the process used here, with $MgTiO_3$ as a precursor combined with a standard sintering technique, can yield BMT-PT with good properties, such as high d_{33} (216 pC/N) and large dielectric breakdown strength (above 8 kV/mm).

As has been demonstrated, BMT-PT is a highly promising high temperature piezoelectric; thanks to several advantages, such as high T_C, high piezoelectric properties, and good thermal stability of poled domains. However, two major aspects warrant future studies. One is to improve resistivity, for example, by using dopants that have been successful in PZT materials,[33] because improved resistivity would permit BMT-PT to be used at even higher temperatures. The other is to understand the correlation between crystal symmetry and piezoelectric properties. An interesting aspect is revealed when the small signal d_{33} value of typical $BiMeO_3-PT$ systems is plotted as a function of the tolerance factor (t) at their MPB as shown in Fig. 9. The rhombohedral component phase at the MPB can either be $R3c$ or $R3m$, which differs with respect to tilted or untilted oxygen octahedra. The tolerance factor (t) at the MPB has a lower value for the tilted $R3c$ phase than for the untilted $R3m$ one. At the moment, the number of data is too small to derive any meaningful correlation between d_{33} and t in $R3c$-based systems, but it is quite evident that the correlation between t and the small signal d_{33} depends significantly on t in $R3m$-based systems. BMT-PT has a MPB consisting of tetragonal ($P4mm$) and rhombohedral ($R3c$) phases.[13] The $R3c$ structure was suggested to be a reason for the low piezoelectric property, because antiphase boundaries associated with oxygen octahedral tilting act as pinning sites at domain boundaries and suppress domain wall mobility.[13,34] The piezoelectric property of BMT-PT could be improved by increasing its tolerance factor at the MPB by suitable doping. The increase in t could convert the rhombohedral structure from $R3c$ to $R3m$, and thus improve the piezoelectric property. In analogy, the piezoelectric property of those MPB with $R3m$ phase may improve by decreasing the t value of the MPB to a critical one where the phase transformation of $R3m$ to $R3c$ takes place. Similar results can also be found in PZT.[35] We expect that a systematic investigation on this topic will lead to a better understanding of the nature of piezoelectricity.

IV. CONCLUSIONS

The ferroelectric and piezoelectric properties of BMT-PT of compositions near the MPB were investigated as a function of temperature from room temperature to 175 °C. It was observed that the maximum and remanent polarizations (P_{max} and P_r) are enhanced with temperature. The increase in the polarization values was explained in terms of the enhanced domain wall mobility due to the reduced lattice distortion at elevated temperatures. This reduced the coercive field and effectively subjected the specimen to higher normalized electric fields. Especially BMT-PT38, which lies at the tetragonal side of the MPB, was found to have a good resistance against thermal depoling above 200 °C, which suggests that tetragonal BMT-PT is promising for high temperature applications.

ACKNOWLEDGMENTS

J.C. thanks the Alexander von Humboldt foundation for financial support.

[1] C. A. Randall, R. E. Eitel, C. Stringer, T. H. Song, S. J. Zhang, and T. R. Shrout, in *High Performance, High Temperature Perovskite Piezoelectric Ceramics in Piezoelectric Single Crystals*, edited by S. Trolier-McKinstry (The Pennsylvania State University, University Park, PA, 2004).
[2] T. R. Shrout, S. J. Zhang, R. Eitel, C. Stringer, and C. A. Randall, Proceedings of the 14th IEEE International Symposium on Applications of

Ferroelectrics, 2004 (unpublished), p. 126.
[3]R. C. Turner, P. A. Fuierer, R. E. Newnham, and T. R. Shrout, Appl. Acoust. **41**, 299 (1994).
[4]T. R. Shrout, R. E. Eitel, and C. A. Randall, in *Piezoelectric Materials in Devices*, edited by N. Setter (EPFL Swiss Federal Institute of Technology, Lausanne, Switzerland, 2002), p. 413.
[5]R. E. Eitel, C. A. Randall, T. R. Shrout, P. W. Rehrig, W. Hackenberger, and S.-E. Park, Jpn. J. Appl. Phys., Part 1 **40**, 5999 (2001).
[6]R. E. Eitel, C. A. Randall, T. R. Shrout, and S.-E. Park, Jpn. J. Appl. Phys., Part 1 **41**, 2099 (2002).
[7]C. J. Stringer, T. R. Shrout, C. A. Randall, and I. M. Reaney, J. Appl. Phys. **99**, 024106 (2006).
[8]M. R. Suchomel and P. K. Davies, J. Appl. Phys. **96**, 4405 (2004).
[9]I. Sterianou, I. M. Reaney, D. C. Sinclair, D. I. Woodward, D. A. Hall, A. J. Bell, and T. P. Comyn, Appl. Phys. Lett. **87**, 242901 (2005).
[10]J. R. Cheng, R. E. Eitel, N. Li, and L. E. Cross, J. Appl. Phys. **94**, 605 (2003).
[11]J. Chen, X. R. Xing, G. R. Liu, J. H. Li, and Y. T. Liu, Appl. Phys. Lett. **89**, 101914 (2006).
[12]S. M. Choi, C. J. Stringer, T. R. Shrout, and C. A. Randall, J. Appl. Phys. **98**, 034108 (2005).
[13]C. A. Randall, R. E. Eitel, B. Jones, T. R. Shrout, D. I. Woodward, and I. M. Reaney, J. Appl. Phys. **95**, 3633 (2004).
[14]A. Moure, M. Algueró, L. Pardo, E. Ringgaard, and A. F. Pedersen, J. Eur. Ceram. Soc. **27**, 237 (2007).
[15]M. D. Snel, W. A. Groen, and G. de With, J. Eur. Ceram. Soc. **25**, 3229 (2005).
[16]J. R. Cheng, Z. Y. Meng, and L. E. Cross, J. Appl. Phys. **96**, 6611 (2004).
[17]M. D. Snel, W. A. Groen, and G. de With, J. Eur. Ceram. Soc. **26**, 89 (2006).
[18]C. J. Stringer, R. E. Eitel, T. R. Shrout, C. A. Randall, and I. M. Reaney, J. Appl. Phys. **97**, 024101 (2005).
[19]S. J. Zhang, C. Stringer, R. Xia, S.-M. Choi, C. A. Randall, and T. R. Shrout, J. Appl. Phys. **98**, 034103 (2005).
[20]M. Kobune, W. Adachi, K. Kitada, A. Mineshige, T. Yazawa, H. Yamaguchi, and K. Honda, Jpn. J. Appl. Phys. **47**, 7664 (2008).
[21]S. J. Zhang, R. Xia, C. A. Randall, and T. R. Shrout, J. Mater. Res. **20**, 2067 (2005).
[22]M. R. Suchomel and P. K. Davies, Appl. Phys. Lett. **86**, 262905 (2005).
[23]J. Chen, X. R. Xing, C. Sun, P. H. Hu, R. B. Yu, X. W. Wang, and L. L. Li, J. Am. Chem. Soc. **130**, 1144 (2008).
[24]S. Nomura, K. Kaneta, J. Kuwata, and K. Uchino, Mater. Res. Bull. **17**, 1471 (1982).
[25]I. Grinberg, M. R. Suchomel, P. K. Davies, and A. M. Rappe, J. Appl. Phys. **98**, 094111 (2005).
[26]S. J. Zhang, C. A. Randall, and T. R. Shrout, Solid State Commun. **131**, 41 (2004).
[27]H. Kungl, R. Theissmann, M. Knapp, C. Baehtz, H. Fuess, S. Wagner, T. Fett, and M. J. Hoffmann, Acta Mater. **55**, 1849 (2007).
[28]R. A. Wolf and S. Trolier-McKinstry, J. Appl. Phys. **95**, 1397 (2004).
[29]S.-T. Zhang, A. B. Kounga, E. Aulbach, W. Jo, T. Granzow, H. Ehrenberg, and J. Rödel, J. Appl. Phys. **103**, 034108 (2008).
[30]T. R. Shrout and S. J. Zhang, J. Electroceram. **19**, 113 (2007).
[31]H. Kungl and M. J. Hoffmann, Acta Mater. **55**, 5780 (2007).
[32]I. Kerkamm, P. Hiller, T. Granzow, and J. Rödel, Acta Mater. **57**, 77 (2009).
[33]M. Takahashi, Jpn. J. Appl. Phys. **10**, 643 (1971).
[34]R. Eitel and C. A. Randall, Phys. Rev. B **75**, 094106 (2007).
[35]H. Zheng, I. M. Reaney, W. E. Lee, N. Jones, and H. Thomas, J. Am. Ceram. Soc. **85**, 2337 (2002).